

Quantized transport of solitons in nonlinear Thouless pumps: From Wannier drags to topological polarons

N. Mostaan,^{1,2,3,*} F. Grusdt,^{1,2} and N. Goldman^{3,†}

¹*Department of Physics and Arnold Sommerfeld Center for Theoretical Physics (ASC),
Ludwig-Maximilians-Universität München, Theresienstr. 37, D-80333 München, Germany*

²*Munich Center for Quantum Science and Technology (MCQST), Schellingstr. 4, D-80799 München, Germany*

³*CENOLI, Université Libre de Bruxelles, CP 231, Campus Plaine, B-1050 Brussels, Belgium*

(Dated: March 11, 2022)

Recent progress in synthetic lattice systems has opened the door to novel explorations of topological matter. In particular, photonics devices and ultracold matter waves offer the unique possibility of studying the rich interplay between topological band structures and tunable nonlinearities. In this emerging field of nonlinear topological physics, a recent experiment [Nature **596**, 63 (2021)] revealed the quantized motion of localized nonlinear excitations, known as solitons, upon driving a Thouless pump sequence; the reported results suggest that the quantized displacement of solitons is dictated by the Chern number of the band from which they emanate. In this Letter, we elucidate the origin of this nonlinear topological effect, by showing that the motion of solitons is established by the quantized displacement of Wannier functions. Furthermore, we consider the quantum-mechanical parent of this setting and relate the quantized motion of solitons to the transport of Bose polarons (dressed impurities). By demonstrating the quantized pumping of Bose polarons, our work introduces a novel instance of topological polaron, which could be observed in ultracold atomic mixtures.

Introduction. Quantized responses have been a central theme throughout the realm of topological physics, which was initiated with the discovery of the quantum Hall effects in two-dimensional electron gases [1, 2]. A wide variety of topological band structures have been revealed over the last decades, leading to the identification of various forms of quantized responses, from quantized Faraday and Kerr rotations in three-dimensional topological insulators [3] to quantized circular dichroism [4] and topological Bloch oscillations [5, 6] in two-dimensional ultracold atomic gases. An emblematic and minimal instance of quantized topological transport concerns the adiabatic motion of a quantum particle moving in a slowly-varying periodic potential, an effect known as the Thouless pump [7]. In this setting, the center-of-mass motion is quantized according to the Chern number of the underlying band structure, as defined over a hybrid momentum-time space [8]. The realization of synthetic lattice systems has allowed for the experimental implementation of Thouless pumps and for the observation of the related quantized motion, in both photonics [9–14] and ultracold gases setups [15, 16].

Interestingly, synthetic topological systems [17, 18] can operate beyond the linear regime of the Schrödinger equation, hence opening the door to nonlinear topological physics [19]. In this emerging framework, a central topic concerns the possible interplay between nonlinear excitations, known as solitons, and the underlying topological band structure [20–31]. Interestingly, exact correspondences between topological indices and nonlinear modes have been identified in mechanical systems [32] and for the Korteweg-de-Vries equation of fluid dynamics [33], hence allowing for a formal topological classification of nonlinear excitations. In the context of nonlinear topological photonics, a recent experimental study reported on the quantized motion of solitons in a lattice system

undergoing a Thouless pump sequence [34]. Despite the presence of considerable nonlinearity, the quantization of the soliton’s displacement was shown to be dictated by the Chern numbers of the underlying band structure.

It is the aim of this Letter to elucidate and explore the quantized transport of solitons in nonlinear topological Thouless pumps. Inspired by the experiment of Ref. [34], we address this topic by setting the focus on a class of one-dimensional systems described by the discrete nonlinear Schrödinger equation (DNLS) [35, 36]. In the regime of weak nonlinearity, solitons are known to predominantly occupy a single Bloch band [36]. Following Ref. [37], we represent the solitons in terms of maximally localized Wannier functions, defined in the corresponding Bloch band. In this Wannier representation, the adiabatic motion of the soliton can be deduced from an ordinary (scalar) DNLS. From this, we show that the quantized motion of the soliton upon pumping is directly related to the quantized displacement of Wannier functions, as established by the Chern number of the band [15, 38, 39]; see Figs. 1(a)-(b).

We then provide a complementary view on this nonlinear topological effect, by considering an instructive mapping to a Bose-polaron setting [40]. This approach builds on the quantum-mechanical description of an interacting bosonic gas, which encompasses the aforementioned NLS as its semiclassical limit. We map the interacting bosonic problem to non-interacting bosons coupled to interacting impurities. This setting gives rise to the formation of Bose polarons, i.e. impurities dressed by bosonic excitations [40–42]. In this picture, the soliton is viewed as a self-trapped Bose polaron, which is shown to undergo quantized motion upon pumping; see Fig. 1(c). This analysis reveals a distinct type of topological polaron [43–48], which arises as a solitonic excitation of a Bose-Bose mixture.

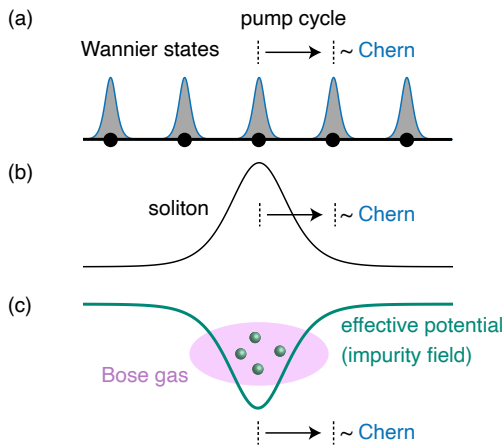


FIG. 1. (a) In a Thouless pump, the Wannier functions perform a quantized drift established by the Chern number of the corresponding band. (b) In a nonlinear setting, the motion of a soliton follows the quantized Wannier drift. (c) Bose polarons, i.e. quantum impurities dressed by bosonic excitations, undergo the same quantized drift upon pumping.

Model and theory. We consider a generic class of lattice models governed by the Discrete Nonlinear Schrödinger equation (DNLS),

$$i\partial_t \phi_i = \sum_{\mathbf{j}} H_{ij}(t) \phi_{\mathbf{j}} - g |\phi_i|^2 \phi_i, \quad (1)$$

where the Hamiltonian $H(t)$ incorporates a slow time-periodic modulation driving a Thouless pump [7, 38]. We label the field ϕ_i , at unit cell i with internal degree of freedom α , using the multi-index $\mathbf{i} = (i, \alpha)$; H_{ij} denotes the Hamiltonian matrix elements between states \mathbf{i} and \mathbf{j} ; and $g > 0$ is the strength of the focusing nonlinearity (attractive self-interaction). The adiabatic evolution is characterized by the period of the pump T , which exceeds all other time scales. Introducing the *adiabatic time* $s = t/T$, Eq. (1) takes the form $i\varepsilon \partial_s \phi_i = \sum_{\mathbf{j}} H_{ij}(s) \phi_{\mathbf{j}} - g |\phi_i|^2 \phi_i$, where $\varepsilon = 1/T$. The solutions to the adiabatic DNLS can be well approximated by stationary states of the form $\phi_i \propto e^{-i\theta_s} \varphi_i$, where θ_s is a time-dependent phase factor and φ_i is an instantaneous solution of the stationary nonlinear Schrödinger equation [49–51]

$$\mu_s \varphi_i = \sum_{\mathbf{j}} H_{ij}(s) \varphi_{\mathbf{j}} - g |\varphi_i|^2 \varphi_i. \quad (2)$$

Eq. (2) admits (bright) solitons as stationary state solutions, which are stable localized structures in the bulk. For sufficiently weak nonlinearity, solitons predominantly occupy the band from which they bifurcate [52], while increasing nonlinearity leads to band mixing. In real space, solitons are immobile without external forcing, and are degenerate modulo a lattice translation set by the translational symmetry of the system. By adiabatically changing the Hamiltonian $H(t)$, a single soliton undergoes smooth deformation, and after one period, it is mapped to the manifold of initial solutions, implying translation by an

integer multiple of the unit cell. According to the observation of Ref. [34], solitons bifurcating from a single Bloch band undergo a quantized displacement dictated by the Chern number of the band [7] over each pump cycle.

To elucidate the mechanism behind this topological nonlinear effect, we follow Ref. [37] and represent the solitons of Eq. (2) in the basis of maximally localized Wannier states,

$$\varphi_i = \sum_n \varphi_i^{(n)}, \quad \varphi_i^{(n)} = \sum_l a_l^{(n)} w_i^{(n)}(l), \quad (3)$$

where the superscript n denotes the occupied band, and the index l labels the unit cell on which the Wannier state is localized. The coefficients $a_l^{(n)}$ obey the analogue of Eq. (2) in the Wannier representation [51]

$$\begin{aligned} \mu_s a_l^{(n)} &= \sum_{l_1} \omega_{l-l_1} a_{l_1}^{(n)} \\ &- g \sum_{n_1, n_2, n_3} \sum_{l_1, l_2, l_3} W_{\underline{l}}^{(n)} a_{l_1}^{(n_1)*} a_{l_2}^{(n_2)} a_{l_3}^{(n_3)}, \end{aligned} \quad (4)$$

where $\omega_l = 1/N \sum_{\mathbf{k}} \exp(ikl) \epsilon_{\mathbf{k}}^{(n)}$ is the Fourier transform of the n th energy band, $\underline{n} = (n, n_1, n_2, n_3)$, $\underline{l} = (l, l_1, l_2, l_3)$, and $W_{\underline{l}}^{(n)}$ are the following Wannier overlaps

$$W_{\underline{l}}^{(n)} = \sum_{\mathbf{j}} w_{\mathbf{j}}^{(n)*}(l) w_{\mathbf{j}}^{(n_1)*}(l_1) w_{\mathbf{j}}^{(n_2)}(l_2) w_{\mathbf{j}}^{(n_3)}(l_3). \quad (5)$$

Wannier states of a band are not unique, as they depend on the gauge choice for the Bloch functions [53]. Nevertheless, a unique set of maximally localized Wannier functions is provided by the eigenstates of the projection of the position operator on the associated band. Since such Wannier functions are exponentially localized, the contribution to the Wannier overlaps in Eq. (5) from Wannier functions corresponding to different unit cells are negligible. The Wannier overlaps can thus be simplified as $W_{\underline{l}}^{(n)} = W^{(n)} \delta_{ll_1} \delta_{l_1 l_2} \delta_{l_2 l_3}$.

Moreover, in the regime of weak nonlinearity, the initial state soliton occupies a single band, which allows us to neglect inter-band contributions to Eq. (4). We note that this simplification holds throughout the evolution of the pump, during which the soliton adiabatically follows the same band.

Under those realistic assumptions, the Wannier representation of the DNLS reduces to the form

$$\mu_s a_l^{(n)} = \sum_{l_1} \omega_{l-l_1} a_{l_1}^{(n)} - g W^{(n)} |a_l^{(n)}|^2 a_l^{(n)}. \quad (6)$$

Eq. (6) has the form of a scalar DNLS on a simple lattice with one degree of freedom per unit cell labeled by Wannier indices l , with hopping terms involving nearest and beyond-nearest neighbors. The properties of such scalar DNLS are well established [36, 54, 55]: Eq. (6) admits inter-site solitons, with maxima on two adjacent sites, and on-site solitons, with their maximum on a single site. The inter-site solitons are known to be unstable against

small perturbations, we thus restrict ourselves to the stable on-site solitons. Crucially, on-site solitons are always peaked around a single site (l) throughout the pumping cycle, as there is a finite energy (Peierls-Naborro) barrier for delocalization [36, 55]. This observation suggests that solitons are dragged by Wannier states upon pumping, hence exhibiting a quantized displacement in real space established by the Chern number [Figs. 1(a)-(b)].

To prove the quantized pumping of solitons, we evaluate their center-of-mass displacement after one period [51]

$$\begin{aligned} \Delta \langle \varphi^{(n)}, X \varphi^{(n)} \rangle &= \Delta \langle w^{(n)}(0), X w^{(n)}(0) \rangle \\ &+ \Delta \sum_{l \neq l'} a_{l'}^{(n)*} a_l^{(n)} \langle w^{(n)}(l'), X w^{(n)}(l) \rangle, \end{aligned} \quad (7)$$

where X is the position operator of the lattice, $\Delta(\cdot) \equiv (\cdot)_{s=1} - (\cdot)_{s=0}$, and $\langle f, g \rangle \equiv \sum_{\mathbf{i}} f_{\mathbf{i}}^* g_{\mathbf{i}}$ is the inner product of fields on the lattice. The first term in Eq. (7) corresponds to the Chern number of the band [51], while the second term is a correction arising due to the finite overlap of different Wannier states. In Ref. [51], we show that this correction term is time periodic and thus does not contribute to the soliton center-of-mass displacement over a pump cycle. This proves that the displacement of the soliton is indeed quantized according to the Chern number of the band from which it emanates.

Numerical validation. We now demonstrate the validity of our assumptions by solving the two-band Rice-Mele model with on-site nonlinearity, which is known to exhibit Thouless pumping in the linear regime ($g=0$) [18, 38]. In Figs. 2(a)-(b), we compare the on-site soliton solution of the simplified Eq. (6), which emerges from the lowest band, with the Wannier representation of the exact soliton obtained by solving the full DNLS in Eq. (2). We then perform a similar comparison in real space, by convolving the soliton of Eq. (6) with the corresponding Wannier states, and by comparing this result to the exact soliton of the original nonlinear Rice-Mele model; see Figs. 2(c)-(d). The perfect agreement validates the description of the soliton in Wannier representation using the ordinary nonlinear Schrödinger equation (6).

We depict the motion of the exact soliton in Fig. 3, as obtained by solving Eq. (2) in the time interval $s \in [0, 2]$, and we compare this trajectory with the drift of its underlying Wannier function (i.e. the Wannier state that contributes the most to the expansion (3)). In order to obtain a contiguous path for the Wannier center, we relabeled the Wannier functions whenever the Wannier centers met discontinuities; this smoothing corresponds to a singular gauge transformation of the corresponding Bloch states, and has no physical implication. Figure 3 indicates that the trajectories of the soliton and Wannier center differ at intermediate times ($s \neq \text{integer}$), which we attribute to cross-Wannier effects [51]; however, this deviation remains small and time-periodic over the whole pump cycle, and does not introduce any (integer) correction to the quantized center-of-mass displacement.

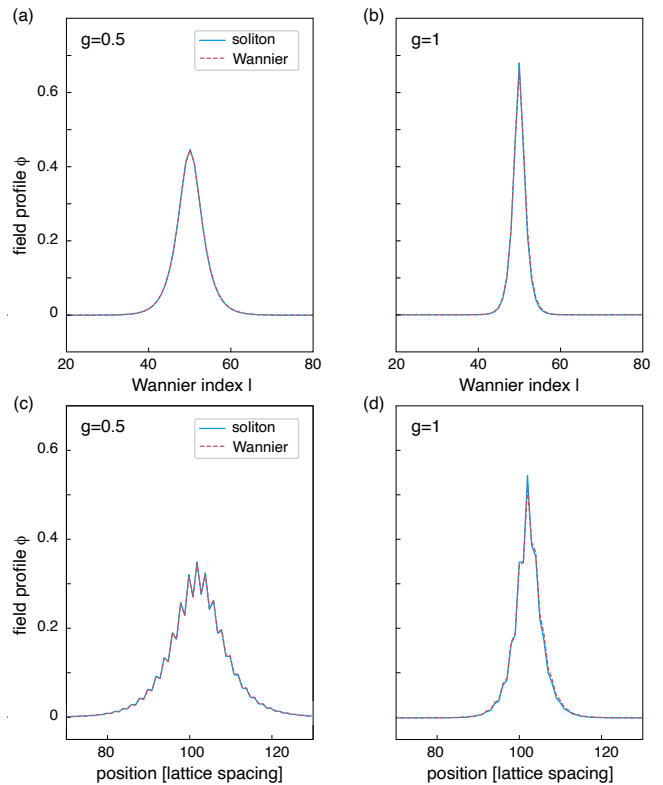


FIG. 2. (a)-(b): Wannier representation of a soliton in the lowest band of the nonlinear Rice-Mele model (blue solid line), compared with the soliton obtained from the simplified DNLS Eq. (6) (dashed red line), for $g = 0.5$ and $g = 1$ and time $s = 0.12$. Note how increasing the nonlinearity further localizes the soliton. (c)-(d) Same comparison in real space.

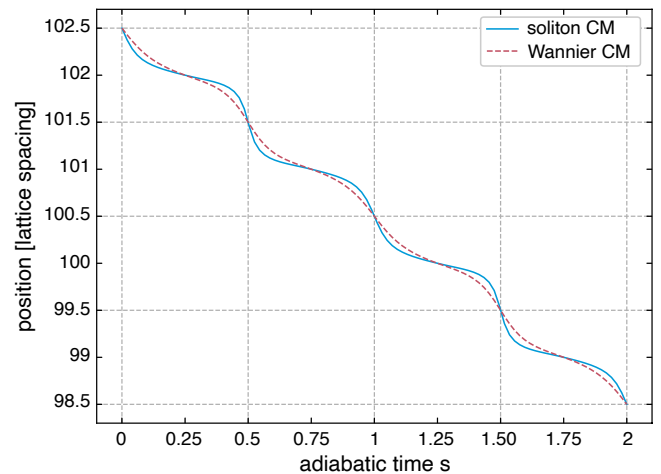


FIG. 3. Adiabatic evolution of the soliton's center-of-mass during two full pump cycles, as obtained by solving Eq. (2) on the Rice-Mele lattice with $g = 0.5$, and selecting a soliton in the lowest band. This is compared to the evolution of the center-of-mass of the Wannier function with largest contribution to the soliton's expansion [Eq. (3)]. For clarity, the Wannier functions are relabeled during the pump cycle such that their center-of-mass follows a contiguous path instead of winding around a unit cell. The quantized displacement is set by the Chern number $C = -1$ of the occupied band.

Relation to topological polarons. We now describe the relevance of these concepts to interacting quantum matter, by relating the quantized motion of solitons to the transport of Bose polarons [40–42]; see Fig. 1(c). This approach reveals a novel form of topological polaron [43–48], which could be probed in ultracold gases.

Let us first remind that the DNLS in Eq. (1) corresponds to the mean-field description of a parent quantum-mechanical system of interacting bosons on a lattice [56]. Formally, the action $S[\bar{\phi}, \phi]$ describing such an interacting bosonic gas is equivalent to the action $\tilde{S}[\bar{\phi}, \phi; u]$ of non-interacting bosons coupled to a real field u [51, 57], hereafter referred to as impurity field. The corresponding impurities are heavy particles (with negligible kinetic energy) and they interact attractively with the bosons; the impurity-impurity interaction is repulsive, which guarantees the stability of the mixture [51]. In this scenario, impurities can form self-trapped bound states by exciting a coherent state of bosonic excitations out of the medium [40–42]. This dressing of impurities by the surrounding bosonic cloud leads to quasiparticles known as Bose polarons [40]. By activating the pump sequence, the bosons drag the heavy impurities, hence leading to the quantized motion of the Bose polaron, as we now demonstrate.

In the semi-classical limit, where the quantum fluctuations of the impurity field are suppressed, one can relate the impurity mean field to the bosonic field as $u_{\text{MF}} = g|\phi|^2$, and the resulting equations of motion read [51]

$$(\mu - (H - u_{\text{MF}}))\phi = 0, \quad u_{\text{MF}} = g|\phi|^2, \quad (8)$$

where H is a free hopping Hamiltonian, and u_{MF} acts as an effective potential for the bosons [Fig. 1(c)]. It appears from Eq. (8) that the self-trapped Bose polaron indeed emerges as the bound state of the impurity field [40–42]. In the context of strong-coupling Bose polaron, it is customary to assume a variational ansatz describing the profile of the impurity field [40]; the bosonic field is then found as the bound state of the impurity potential u_{MF} using the first relation in Eq. (8). Here, the variational problem for obtaining u_{MF} reduces to one for ϕ , because of the constraint $u_{\text{MF}} = g|\phi|^2$. As before, we express ϕ in the Wannier basis, and the variational problem is then solved simultaneously for both u_{MF} and ϕ using the ansatz $a_l = \eta \text{sech}(\xi(l - l_0))$ for the Wannier coefficients of ϕ . The bound state of the resulting impurity potential $u_{\text{MF}} = g|\phi|^2$ then corresponds to the Bose polaron [51].

Figures 4(a) and (b) show the adiabatic evolution of the amplitude η and width ξ of the variational solution ϕ . We compare these results with the amplitude and width extracted from the bound-state solution associated with the impurity potential $u_{\text{MF}} = g|\phi|^2$, as well as to those extracted from the exact soliton of Eq. (2) expressed in Wannier representation. We also show the dependence of these parameters on the nonlinearity g in Fig. 4(c), for both the exact soliton and the variational solution. These results validate our variational approach, as well as the bound-state picture of our Bose polaron.

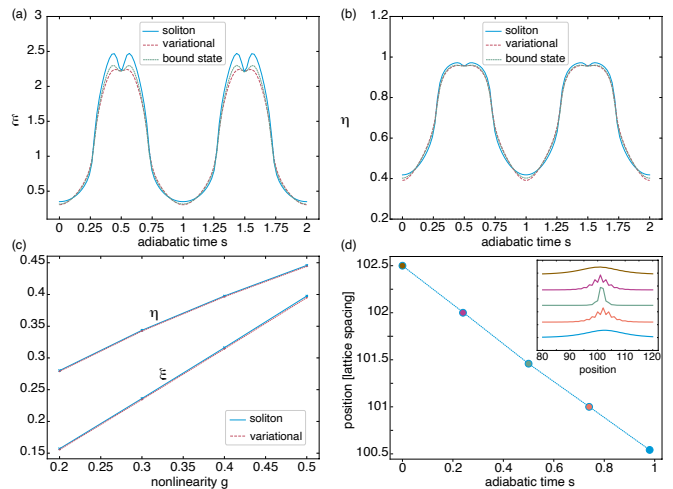


FIG. 4. (a) Evolution of the soliton’s width ξ in Wannier space over two pump cycles, as obtained by fitting the numerical solution of Eq. (2) with a sech function (blue solid line). This is compared to the width of the variational-ansatz solution (dashed red line), and to that of the bound-state solution (green dotted line); here $g = 0.5$. (b) Same for the amplitude η . (c) Amplitude and width of the exact (solid blue line) and variational-ansatz (dashed red line) solutions as a function of g , at time $s = 0.12$. (d) Center-of-mass displacement of the calculated bound state (Bose polaron) over one pump cycle. The inset shows the corresponding bound state profiles. The quantized motion is dictated by the Chern number $C = -1$; compare with Fig. 3.

The minimum-energy solutions obtained from the variational ansatz are realized for integer values of the Wannier index l_0 , and thus correspond to stable on-site solitons. Moreover, this Wannier index l_0 remains constant over a pump cycle. Hence, this suggests that the real-space motion of the Bose polaron should follow the quantized Wannier drift, as established by the Chern number. This is verified in Fig. 4(d), where the center-of-mass displacement of the calculated bound state is shown to be quantized over a pump cycle (compare with Fig. 3).

Our results indicate the possibility of observing topological pumping in impurity-boson mixtures through the formation of localized stable structures. Probing topological properties by forming topological polarons has been proposed earlier, based on binding individual topological excitations to impurities [43, 44, 46, 48]. The present scheme extends those concepts to more complex boson-impurity states.

Implementation. The topological polaron revealed in this work could be explored in ultracold atomic mixtures [58, 59], upon imposing proper interactions among the two species [51]. We propose to use a dual-species BEC in an optical lattice, with strong inter-species interactions, and to apply a pump sequence [15, 16] for the majority atoms. Once implemented, the quantized transport of the Bose polaron can be measured in-situ. The Chern number of the topological Bose polaron could also be directly extracted by interferometry [44].

During the preparation of this manuscript, the authors became aware of a related work by M. Jürgensen and M. C. Rechtsman [60].

Acknowledgement. The authors acknowledge B. Oblak, N. Englebert, S.-P. Gorza, F. Leo, M. Jürgensen, S. Mukherjee and M. C. Rechtsman for useful discussions. Work in Brussels is supported by the FRS-FNRS (Belgium) and the ERC Starting Grant TopoCold. The authors acknowledge funding by the Deutsche Forschungsgemeinschaft (DFG, German Research Foundation) under Germany’s Excellence Strategy – EXC-2111 – 390814868 and via Research Unit FOR 2414 under project number 277974659.

* Nader.Mostaan@physik.uni-muenchen.de

† ngoldman@ulb.ac.be

- [1] M. Z. Hasan and C. L. Kane, “Colloquium: topological insulators,” *Reviews of modern physics*, vol. 82, no. 4, p. 3045, 2010.
- [2] X.-L. Qi and S.-C. Zhang, “Topological insulators and superconductors,” *Reviews of Modern Physics*, vol. 83, no. 4, p. 1057, 2011.
- [3] L. Wu, M. Salehi, N. Koirala, J. Moon, S. Oh, and N. Armitage, “Quantized Faraday and Kerr rotation and axion electrodynamics of a 3d topological insulator,” *Science*, vol. 354, no. 6316, pp. 1124–1127, 2016.
- [4] L. Asteria, D. T. Tran, T. Ozawa, M. Tarnowski, B. S. Rem, N. Fläschner, K. Sengstock, N. Goldman, and C. Weitenberg, “Measuring quantized circular dichroism in ultracold topological matter,” *Nature physics*, vol. 15, no. 5, pp. 449–454, 2019.
- [5] T. Li, L. Duca, M. Reitter, F. Grusdt, E. Demler, M. Endres, M. Schleier-Smith, I. Bloch, and U. Schneider, “Bloch state tomography using Wilson lines,” *Science*, vol. 352, no. 6289, pp. 1094–1097, 2016.
- [6] J. Hoeller and A. Alexandradinata, “Topological Bloch oscillations,” *Physical Review B*, vol. 98, no. 2, p. 024310, 2018.
- [7] D. J. Thouless, “Quantization of particle transport,” *Phys. Rev. B*, vol. 27, pp. 6083–6087, May 1983.
- [8] D. Xiao, M.-C. Chang, and Q. Niu, “Berry phase effects on electronic properties,” *Reviews of modern physics*, vol. 82, no. 3, p. 1959, 2010.
- [9] Y. E. Kraus, Y. Lahini, Z. Ringel, M. Verbin, and O. Zilberberg, “Topological states and adiabatic pumping in quasicrystals,” *Physical review letters*, vol. 109, no. 10, p. 106402, 2012.
- [10] M. Verbin, O. Zilberberg, Y. Lahini, Y. E. Kraus, and Y. Silberberg, “Topological pumping over a photonic fibonacci quasicrystal,” *Physical Review B*, vol. 91, no. 6, p. 064201, 2015.
- [11] O. Zilberberg, S. Huang, J. Guglielmon, M. Wang, K. P. Chen, Y. E. Kraus, and M. C. Rechtsman, “Photonic topological boundary pumping as a probe of 4d quantum hall physics,” *Nature*, vol. 553, no. 7686, pp. 59–62, 2018.
- [12] I. H. Grinberg, M. Lin, C. Harris, W. A. Benalcazar, C. W. Peterson, T. L. Hughes, and G. Bahl, “Robust temporal pumping in a magneto-mechanical topological insulator,” *Nature communications*, vol. 11, no. 1, pp. 1–9, 2020.
- [13] A. Cerjan, M. Wang, S. Huang, K. P. Chen, and M. C. Rechtsman, “Thouless pumping in disordered photonic systems,” *Light: Science & Applications*, vol. 9, no. 1, pp. 1–7, 2020.
- [14] Y. Ke, X. Qin, F. Mei, H. Zhong, Y. S. Kivshar, and C. Lee, “Topological phase transitions and Thouless pumping of light in photonic waveguide arrays,” *Laser & Photonics Reviews*, vol. 10, no. 6, pp. 995–1001, 2016.
- [15] M. Lohse, C. Schweizer, O. Zilberberg, M. Aidelsburger, and I. Bloch, “A Thouless quantum pump with ultracold bosonic atoms in an optical superlattice,” *Nature Physics*, vol. 12, no. 4, pp. 350–354, 2016.
- [16] S. Nakajima, T. Tomita, S. Taie, T. Ichinose, H. Ozawa, L. Wang, M. Troyer, and Y. Takahashi, “Topological Thouless pumping of ultracold fermions,” *Nature Physics*, vol. 12, no. 4, pp. 296–300, 2016.
- [17] T. Ozawa, H. M. Price, A. Amo, N. Goldman, M. Hafezi, L. Lu, M. C. Rechtsman, D. Schuster, J. Simon, O. Zilberberg, *et al.*, “Topological photonics,” *Reviews of Modern Physics*, vol. 91, no. 1, p. 015006, 2019.
- [18] N. Cooper, J. Dalibard, and I. Spielman, “Topological bands for ultracold atoms,” *Reviews of modern physics*, vol. 91, no. 1, p. 015005, 2019.
- [19] D. Smirnova, D. Leykam, Y. Chong, and Y. Kivshar, “Nonlinear topological photonics,” *Applied Physics Reviews*, vol. 7, no. 2, p. 021306, 2020.
- [20] D. Leykam and Y. D. Chong, “Edge solitons in nonlinear-photonic topological insulators,” *Physical review letters*, vol. 117, no. 14, p. 143901, 2016.
- [21] D. Solnyshkov, O. Bleu, B. Teklu, and G. Malpuech, “Chirality of topological gap solitons in bosonic dimer chains,” *Physical review letters*, vol. 118, no. 2, p. 023901, 2017.
- [22] P. St-Jean, V. Goblot, E. Galopin, A. Lemaître, T. Ozawa, L. Le Gratiet, I. Sagnes, J. Bloch, and A. Amo, “Lasing in topological edge states of a one-dimensional lattice,” *Nature Photonics*, vol. 11, no. 10, pp. 651–656, 2017.
- [23] A. Bisianov, M. Wimmer, U. Peschel, and O. Egorov, “Stability of topologically protected edge states in nonlinear fiber loops,” *Physical Review A*, vol. 100, no. 6, p. 063830, 2019.
- [24] S. K. Ivanov, Y. V. Kartashov, A. Szameit, L. Torner, and V. V. Konotop, “Vector topological edge solitons in Floquet insulators,” *ACS Photonics*, vol. 7, no. 3, pp. 735–745, 2020.
- [25] D. González-Cuadra, A. Dauphin, P. R. Grzybowski, M. Lewenstein, and A. Bermudez, “Dynamical solitons and boson fractionalization in cold-atom topological insulators,” *Physical Review Letters*, vol. 125, no. 26, p. 265301, 2020.
- [26] S. Mukherjee and M. C. Rechtsman, “Observation of Floquet solitons in a topological bandgap,” *Science*, vol. 368, no. 6493, pp. 856–859, 2020.
- [27] S. Mukherjee and M. C. Rechtsman, “Observation of unidirectional soliton-like edge states in nonlinear floquet topological insulators,” *arXiv preprint arXiv:2010.11359*, 2020.
- [28] S. Xia, D. Jukić, N. Wang, D. Smirnova, L. Smirnov, L. Tang, D. Song, A. Szameit, D. Leykam, J. Xu, *et al.*, “Nontrivial coupling of light into a defect: the interplay of nonlinearity and topology,” *Light: Science & Applications*, vol. 9, no. 1, pp. 1–10, 2020.

- [29] N. Pernet, P. St-Jean, D. Solnyshkov, G. Malpuech, N. C. Zambon, B. Real, O. Jamadi, A. Lemaître, M. Morassi, L. L. Gratiet, *et al.*, “Topological gap solitons in a 1d non-hermitian lattice,” *arXiv preprint arXiv:2101.01038*, 2021.
- [30] S. Mittal, G. Moille, K. Srinivasan, Y. K. Chembo, and M. Hafezi, “Topological frequency combs and nested temporal solitons,” *arXiv preprint arXiv:2101.02229*, 2021.
- [31] M. S. Kirsch, Y. Zhang, M. Kremer, L. J. Maczewsky, S. K. Ivanov, Y. V. Kartashov, L. Torner, D. Bauer, A. Szameit, and M. Heinrich, “Nonlinear second-order photonic topological insulators,” *arXiv preprint arXiv:2104.13112*, 2021.
- [32] P.-W. Lo, C. D. Santangelo, B. G.-g. Chen, C.-M. Jian, K. Roychowdhury, and M. J. Lawler, “Topology in nonlinear mechanical systems,” *Physical Review Letters*, vol. 127, no. 7, p. 076802, 2021.
- [33] B. Oblak and G. Kozyreff, “Berry phases in the reconstructed KDV equation,” *Chaos: An Interdisciplinary Journal of Nonlinear Science*, vol. 30, no. 11, p. 113114, 2020.
- [34] M. Jürgensen, S. Mukherjee, and M. C. Rechtsman, “Quantized nonlinear Thouless pumping,” *Nature*, vol. 596, no. 7870, pp. 63–67, 2021.
- [35] C. Sulem and P. Sulem, *The Nonlinear Schrödinger Equation*. Springer-Verlag New York, 1999.
- [36] P. G. Kevrekidis, *The discrete nonlinear Schrödinger equation: mathematical analysis, numerical computations and physical perspectives*, vol. 232. Springer Science & Business Media, 2009.
- [37] G. Alfimov, P. Kevrekidis, V. Konotop, and M. Salerno, “Wannier functions analysis of the nonlinear Schrödinger equation with a periodic potential,” *Physical Review E*, vol. 66, no. 4, p. 046608, 2002.
- [38] J. K. Asbóth, L. Oroszlány, and A. Pályi, “A short course on topological insulators,” *Lecture notes in physics*, vol. 919, p. 166, 2016.
- [39] F. Mei, J.-B. You, D.-W. Zhang, X. Yang, R. Fazio, S.-L. Zhu, and L. C. Kwek, “Topological insulator and particle pumping in a one-dimensional shaken optical lattice,” *Physical Review A*, vol. 90, no. 6, p. 063638, 2014.
- [40] F. Grusdt and E. Demler, “New theoretical approaches to Bose polarons,” *Quantum Matter at Ultralow Temperatures*, vol. 191, p. 325, 2015.
- [41] L. Landau and S. Pekar, “Effective mass of a polaron,” *Zh. Eksp. Teor. Fiz.*, vol. 18, no. 5, pp. 419–423, 1948.
- [42] J. Devreese, “Fröhlich polarons. Lecture course including detailed theoretical derivations,” *arXiv e-prints*, pp. arXiv–1012, 2010.
- [43] F. Grusdt, N. Y. Yao, D. Abanin, M. Fleischhauer, and E. Demler, “Interferometric measurements of many-body topological invariants using mobile impurities,” *Nature communications*, vol. 7, no. 1, pp. 1–9, 2016.
- [44] F. Grusdt, N. Y. Yao, and E. Demler, “Topological polarons, quasiparticle invariants, and their detection in one-dimensional symmetry-protected phases,” *Physical Review B*, vol. 100, no. 7, p. 075126, 2019.
- [45] A. Camacho-Guardian, N. Goldman, P. Massignan, and G. M. Bruun, “Dropping an impurity into a chern insulator: A polaron view on topological matter,” *Physical Review B*, vol. 99, no. 8, p. 081105, 2019.
- [46] A. M. de las Heras, E. Macaluso, and I. Carusotto, “Anyonic molecules in atomic fractional quantum Hall liquids: a quantitative probe of fractional charge and anyonic statistics,” *Physical Review X*, vol. 10, no. 4, p. 041058, 2020.
- [47] D. Pimenov, A. Camacho-Guardian, N. Goldman, P. Massignan, G. Bruun, and M. Goldstein, “Topological transport of mobile impurities,” *Physical Review B*, vol. 103, no. 24, p. 245106, 2021.
- [48] N. Baldelli, B. Juliá-Díaz, U. Bhattacharya, M. Lewenstein, and T. Graß, “Tracing non-Abelian anyons via impurity particles,” *Phys. Rev. B*, vol. 104, p. 035133, Jul 2021.
- [49] Z. Gang and P. Grech, “Adiabatic theorem for the Gross–Pitaevskii equation,” *Communications in Partial Differential Equations*, vol. 42, no. 5, pp. 731–756, 2017.
- [50] R. Carles and C. Sparber, “Semiclassical wave packet dynamics in Schrödinger equations with periodic potentials,” *arXiv preprint arXiv:1101.3136*, 2011.
- [51] See Supplementary Material for details on: the adiabatic theorem for NLS, the Rice-Mele model and pump sequence, the derivation of the scalar DNLS, the relation between impurity-boson mixtures and solitons, the variational ansatz for the state of the topological polaron, and the derivation of the soliton center-of-mass displacement.
- [52] A. Szameit and S. Nolte, “Discrete optics in femtosecond-laser-written photonic structures,” *Journal of Physics B: Atomic, Molecular and Optical Physics*, vol. 43, no. 16, p. 163001, 2010.
- [53] R. Yu, X. L. Qi, A. Bernevig, Z. Fang, and X. Dai, “Equivalent expression of Z2 topological invariant for band insulators using the non-Abelian Berry connection,” *Physical Review B*, vol. 84, no. 7, p. 075119, 2011.
- [54] P. G. Kevrekidis, Y. S. Kivshar, and A. S. Kovalev, “Instabilities and bifurcations of nonlinear impurity modes,” *Physical Review E*, vol. 67, no. 4, p. 046604, 2003.
- [55] Y. S. Kivshar and D. K. Campbell, “Peierls-Nabarro potential barrier for highly localized nonlinear modes,” *Physical Review E*, vol. 48, no. 4, p. 3077, 1993.
- [56] A. Polkovnikov, S. Sachdev, and S. Girvin, “Nonequilibrium Gross-Pitaevskii dynamics of boson lattice models,” *Physical Review A*, vol. 66, no. 5, p. 053607, 2002.
- [57] H. T. Stoof, K. B. Gubbels, and D. B. Dickerscheid, *Ultracold quantum fields*, vol. 1. Springer, 2009.
- [58] I. Bloch, J. Dalibard, and W. Zwerger, “Many-body physics with ultracold gases,” *Reviews of modern physics*, vol. 80, no. 3, p. 885, 2008.
- [59] C. Chin, R. Grimm, P. Julienne, and E. Tiesinga, “Feshbach resonances in ultracold gases,” *Reviews of Modern Physics*, vol. 82, no. 2, p. 1225, 2010.
- [60] M. Jürgensen and M. C. Rechtsman, “The Chern number governs soliton motion in nonlinear Thouless pumps,” *arXiv preprint arXiv:2110.08696*, 2021.
- [61] J. Jager, R. Barnett, M. Will, and M. Fleischhauer, “Strong-coupling bose polarons in one dimension: Condensate deformation and modified Bogoliubov phonons,” *Physical Review Research*, vol. 2, no. 3, p. 033142, 2020.

**SUPPLEMENTARY MATERIAL FOR:
QUANTIZED TRANSPORT OF SOLITONS IN NONLINEAR THOULESS PUMPS:
FROM WANNIER DRAGS TO TOPOLOGICAL POLARONS**

N. Mostaan,^{1,2,3} F. Grusdt,^{1,2} N. Goldman,³

¹*Department of Physics and Arnold Sommerfeld Center for Theoretical Physics (ASC),
Ludwig-Maximilians-Universität München, Theresienstr. 37, D-80333 München, Germany*

²*Munich Center for Quantum Science and Technology (MCQST), Schellingstr. 4, D-80799 München, Germany*

³*CENOLI, Université Libre de Bruxelles, CP 231, Campus Plaine, B-1050 Brussels, Belgium*

ADIABATIC THEOREM FOR NLS

The adiabatic theorem for NLS (both continuous and discrete forms), follows closely the formulation of its linear counterpart [49, 50]. For a system with time-dependent Hamiltonian $H(t)$ which varies on a time scale T much larger than all the time scales in the problem, the time-dependent NLS in terms of the adiabatic time $s = t/T$ and the rate of change $\varepsilon = 1/T$ takes the following form,

$$i\varepsilon \partial_s \phi = H(s) \phi - g|\phi|^2 \phi, \quad (\text{S9})$$

(see the main text). The stationary state solutions of Eq. (S9) are of the form

$$\phi_s = e^{-i\theta_s} (\varphi_s + \delta \varphi_s), \quad (\text{S10})$$

where φ_s is the instantaneous solution of the stationary NLS,

$$\mu_s \varphi_s = H(s) \varphi_s - g|\varphi_s|^2 \varphi_s, \quad (\text{S11})$$

and $\theta_s = 1/\varepsilon (\int_0^s ds' \mu_{s'} - \gamma_s)$ is a global phase factor consisting of a dynamical contribution and a Berry phase, and it can be ignored. The correction term $\delta \varphi_s$ accounts for non-adiabatic variations, and for $\varepsilon \rightarrow 0$, it behaves as $|\delta \varphi| \sim \varepsilon$, hence vanishes in the adiabatic limit $\varepsilon \rightarrow 0$. The relevant dynamical information is therefore encoded in the instantaneous solutions of Eq. (S11).

THE RICE-MELE MODEL AND PUMP SEQUENCE

In the main text, we illustrated the general concepts and results based on the Rice-Mele model, using periodic boundary conditions. This simple two-band model, which is reviewed in some detail below, is known to exhibit a topological (Thouless) pump sequence.

The Rice-Mele model is a 1D tight-binding model with alternating nearest-neighbor tunneling matrix elements (t, t', t, t', \dots), and a staggered on-site potential. We denote the two sites within each unit cell by $\alpha = A, B$ and the unit cells by $i, 0 \leq i \leq N-1$, where N is the number of unit cells. The hopping matrix element between sites A and B within each unit cell (resp. between adjacent unit cells) equals $-t(1+\delta)$ (resp. $-t(1-\delta)$) and the magnitude of the staggered potential on site A (B) equals Δ ($-\Delta$). The Hamiltonian of the Rice-Mele model thus reads as

$$H = -t \sum_{i=0}^{N-1} \left[(1+\delta) |i, A\rangle \langle i, B| + (1-\delta) |i, A\rangle \langle i-1, B| \right] + \frac{\Delta}{2} \sum_{i=0}^{N-1} \left[|i, A\rangle \langle i, A| - |i, B\rangle \langle i, B| \right] + \text{h.c.} \quad (\text{S12})$$

We performed the simulations shown in the main text on a lattice with $N = 100$ unit cells, and the following pump sequence

$$\begin{aligned} t &= t_0 (1 + 1/2 \cos(2\pi s)), \\ \delta &= \delta_0 \cos(2\pi s) / (2 + \cos(2\pi s)), \\ \Delta &= 2 t_0 \sin(2\pi s) / (2 + \cos(2\pi s)), \end{aligned} \quad (\text{S13})$$

with $t_0 = 0.5$ and $\delta_0 = 0.6$. The *nonlinear* Rice-Mele model, which is used in our simulations, is obtained by adding an on-site nonlinearity (see Eq. (1) in the main text) to the lattice model described in this Appendix.

DERIVATION OF THE SCALAR DNLS

In this section we outline the derivation of the simplified scalar DNLS from the original lattice DNLS,

$$\mu \phi_{\mathbf{i}} = \sum_{\mathbf{j}} H_{\mathbf{ij}} \phi_{\mathbf{j}} - g |\phi_{\mathbf{i}}|^2 \phi_{\mathbf{i}}. \quad (\text{S14})$$

The Wannier functions are related to the Bloch waves of the Hamiltonian by the following relations

$$w_{\mathbf{j}}^{(n)}(l) = \frac{1}{\sqrt{N}} \sum_{\mathbf{k}=0}^{N-1} e^{i(2\pi/N)\mathbf{k}(-l)} \psi_{\mathbf{j}}^{(n)}(\mathbf{k}) = \frac{1}{\sqrt{N}} \sum_{\mathbf{k}=0}^{N-1} e^{i(2\pi/N)\mathbf{k}(j-l)} u_{\mathbf{j}}^{(n)}(\mathbf{k}), \quad (\text{S15})$$

where $\psi_{\mathbf{j}}^{(n)}(\mathbf{k}) = e^{i(2\pi/N)\mathbf{k}(j)} u_{\mathbf{j}}^{(n)}(\mathbf{k})$ is the Bloch wave of band n with momentum \mathbf{k} and $u_{\mathbf{j}}^{(n)}(\mathbf{k})$ is the corresponding Bloch function, which is periodic over the unit cells and does not depend on j . To represent the Hamiltonian part in Wannier basis, we evaluate the matrix elements of the Hamiltonian over the Wannier states

$$\begin{aligned} \langle w^{(n')}(l'), H w^{(n)}(l) \rangle &= \frac{1}{N} \sum_{\mathbf{k}, \mathbf{k}'=0}^{N-1} e^{i(2\pi/N)(\mathbf{k}'l' - \mathbf{k}l)} \langle \psi^{(n')}(\mathbf{k}'), H \psi^{(n)}(\mathbf{k}) \rangle \\ &= \frac{1}{N} \sum_{\mathbf{k}, \mathbf{k}'=0}^{N-1} e^{i(2\pi/N)(\mathbf{k}'l' - \mathbf{k}l)} \delta_{nn'} \delta_{\mathbf{k}\mathbf{k}'} \epsilon_{\mathbf{k}}^{(n)} \\ &= \delta_{nn'} \cdot \frac{1}{N} \sum_{\mathbf{k}=0}^{N-1} e^{i(2\pi/N)\mathbf{k}(l'-l)} \epsilon_{\mathbf{k}}^{(n)} = \delta_{nn'} \cdot \omega_{l'-l}, \end{aligned} \quad (\text{S16})$$

where $\omega_l = 1/N \sum_{\mathbf{k}=0}^{N-1} e^{i(2\pi/N)\mathbf{k}l} \epsilon_{\mathbf{k}}^{(n)}$ is the Fourier transform of $\epsilon_{\mathbf{k}}^{(n)}$, see the main text.

Next, we express the nonlinearity in terms of Wannier functions,

$$\langle w^{(n)}(l), |\phi|^2 \phi \rangle = \sum_{n_1, n_2, n_3} \sum_{l_1, l_2, l_3} \left(\sum_{\mathbf{i}} w_{\mathbf{i}}^{(n_1)*}(l) w_{\mathbf{i}}^{(n_1)*}(l_1) w_{\mathbf{i}}^{(n_2)}(l_2) w_{\mathbf{i}}^{(n_3)}(l_3) \right) a_{l_1}^{(n_1)*} a_{l_2}^{(n_2)} a_{l_3}^{(n_3)}. \quad (\text{S17})$$

Taking the inner product of Eq. (S14) with $w_l^{(n)}$ and using Eqs. (S16) and (S17), we obtain the following DNLS

$$\begin{aligned} \mu_s a_l^{(n)} &= \sum_{l_1} \omega_{l-l_1} a_{l_1}^{(n)} \\ &\quad - g \sum_{n_1, n_2, n_3} \sum_{l_1, l_2, l_3} W_l^{(n)} a_{l_1}^{(n_1)*} a_{l_2}^{(n_2)} a_{l_3}^{(n_3)}. \end{aligned} \quad (\text{S18})$$

RELATION BETWEEN IMPURITY-BOSON MIXTURES AND SOLITONS

In the main text, we discussed the possibility of observing a topological pumping effect in ultracold two-species bosonic mixtures, where a stable localized soliton-like structure can be realized, in direct analogy with the soliton pumping of a NLS equation. Note that one does not require mixtures to produce solitons (and the related pumping sequence) in ultracold quantum matter. However, our purpose here is to use the topological soliton pump as a motivation to expand this paradigm to the general setting of ultracold bosonic mixtures, where localized stable structures (not necessarily solitons) with a single band occupation can potentially be generated and be driven through a pumping sequence. As a proof of concept, we demonstrate on a toy model that the microscopic Hamiltonian of an impurity-boson system can, under certain conditions, lead to effective Hamiltonians describing interacting bosonic systems on a mean-field level such as the ones described by the Gross-Pitaevskii equation, and thus mimicking their nonlinear excitations such as bright solitons.

In the following, we start from a microscopic Hamiltonian of an impurity-boson mixture, and we consider stationary state field profiles that minimize the Lagrangian of the action upon neglecting the kinetic energy of the impurities. In the semi-classical limit, we derive equations of motion that closely resemble a NLS equation, which is known to admit bright soliton solutions. This is the demonstration of how an impurity-boson system can lead to similar physics as interacting bosonic systems, and it is at the core of the topological Bose polaron discussed in the main text.

We consider impurities immersed in a bath of non-interacting bosons on a lattice with attractive impurity-boson coupling and repulsive impurity-impurity interaction. For simplicity, the impurity species is considered bosonic as well. The system is described by the following Hamiltonian

$$H = \sum_{\langle i,j \rangle} \phi_i^\dagger H_{ij}^{(\phi)} \phi_j - g_{IB} \sum_i \phi_i^\dagger \phi_i \sigma_i^\dagger \sigma_i + \sum_{\langle i,j \rangle} \sigma_i^\dagger H_{ij}^{(\sigma)} \sigma_j + \frac{1}{2g} \sum_i \sigma_i^\dagger \sigma_i^\dagger \sigma_i \sigma_i. \quad (\text{S19})$$

Here, ϕ_i and σ_i denote boson and impurity fields, respectively, $H_{ij}^{(\phi)} \sim t_\phi$ and $H_{ij}^{(\sigma)} \sim t_\sigma$ are hopping matrix elements of free boson and impurity Hamiltonians with strength t_ϕ and t_σ , respectively, g_{IB} is the strength of the attractive impurity-boson interaction, and $1/g$ is the strength of the repulsive impurity-impurity interaction. We further assume that $g_{IB} = 1$ as it can be set so by a redefinition of the impurity field, g and the impurity Hamiltonian. The coherent-state action of the system thus takes the following form ($\hbar = 1$),

$$S[\bar{\phi}, \phi; \bar{\sigma}, \sigma] = \int_{t_i}^{t_f} dt L[\bar{\phi}, \phi; \bar{\sigma}, \sigma], \quad (\text{S20})$$

with the Lagrangian

$$\begin{aligned} L[\bar{\phi}, \phi; \bar{\sigma}, \sigma] &= \sum_i \bar{\phi}_i [i\partial_t + \mu_\phi] \phi_i - \sum_{\langle i,j \rangle} \bar{\phi}_i H_{ij}^{(\phi)} \phi_j \\ &+ \sum_i \bar{\sigma}_i [i\partial_t + \mu_\sigma + \phi_i^\dagger \phi_i] \sigma_i - \sum_{\langle i,j \rangle} \bar{\sigma}_i H_{ij}^{(\sigma)} \sigma_j - \frac{1}{2g} \sum_i (\sigma_i^\dagger \sigma_i)^2. \end{aligned} \quad (\text{S21})$$

To proceed, we seek stationary state solutions for the coherent state fields of the form $\phi_i^0(t) = e^{-i\omega_0 t} \phi_i^0$ and $\sigma_i^0(t) = e^{-i\omega_0 t} \sigma_i^0$ which minimize $L[\bar{\phi}, \phi; \bar{\sigma}, \sigma]$. Such solutions are the saddle-point solutions of the quantum mechanical action, giving the mean-field stable states of the system. The Lagrangian then takes the time-independent form

$$\begin{aligned} L[\bar{\phi}^0, \phi^0; \bar{\sigma}^0, \sigma^0] &= \sum_i \bar{\phi}_i^0 [\omega_0 + \mu_\phi] \phi_i^0 - \sum_{\langle i,j \rangle} \bar{\phi}_i^0 H_{ij}^{(\phi)} \phi_j^0 \\ &+ \sum_i \bar{\sigma}_i^0 [\omega_0 + \mu_\sigma + \bar{\phi}_i^0 \phi_i^0] \sigma_i^0 - \sum_{\langle i,j \rangle} \bar{\sigma}_i^0 H_{ij}^{(\sigma)} \sigma_j^0 - \frac{1}{2g} \sum_i (\bar{\sigma}_i^0 \sigma_i^0)^2. \end{aligned} \quad (\text{S22})$$

To minimize the Lagrangian, the corresponding Euler-Lagrange equations are derived by $\delta L/\delta \bar{\phi}_i = 0$, and $\delta L/\delta \bar{\sigma}_i = 0$ as the following

$$(\omega_0 + \mu_\phi) \phi_i^0 - \sum_j H_{ij}^{(\phi)} \phi_j^0 + (\bar{\sigma}_i^0 \sigma_i^0) \phi_i^0 = 0, \quad (\text{S23})$$

$$(\omega_0 + \mu_\sigma) \sigma_i^0 - \sum_j H_{ij}^{(\sigma)} \sigma_j^0 + \left(\bar{\phi}_i^0 \phi_i^0 - \frac{1}{g} \bar{\sigma}_i^0 \sigma_i^0 \right) \sigma_i^0 = 0. \quad (\text{S24})$$

In the strong-coupling regime and for heavy impurities, when the strength of the impurity-boson interaction far exceeds the kinetic energy of the impurity as well as typical values for impurity energy $\omega_0 + \mu_\sigma$, the first two terms in Eq. (S24) can be neglected compared to the individual terms in the parentheses. The Eqs. (S23) and (S24) then reduce to

$$(\omega_0 + \mu_\phi) \phi_i^0 - \sum_j H_{ij}^{(\phi)} \phi_j^0 + (\bar{\sigma}_i^0 \sigma_i^0) \phi_i^0 = 0, \quad (\text{S25})$$

$$\bar{\sigma}_i^0 \sigma_i^0 = g \bar{\phi}_i^0 \phi_i^0. \quad (\text{S26})$$

Defining the impurity density profile $u_i^0 = \bar{\sigma}_i^0 \sigma_i^0$, Eqs. (S25) and (S26) yield Eq. (8) in the main text. Note that Eq. (S26) corresponds to a Thomas-Fermi profile of the impurity species, self trapped by its interaction with the majority particles.

We note that our scheme requires a hierarchy of energy scales $t_\sigma \ll t_\phi \sim 1 \ll 1/g$ to implement the analogue of an interacting Bose gas with weak nonlinearities.

VARIATIONAL ANSATZ FOR THE STATE OF THE TOPOLOGICAL POLARON

When a single quantum impurity is immersed in a BEC, it excites a coherent cloud of phonons with which it interacts attractively. In the strong-coupling regime a significant increase of the polaron effective mass occurs, which leads to much slower dynamics of the impurity compared to the phonons, thus a treatment of the dynamics based on Born-Oppenheimer approximation works well [40, 41] (see also [61] for a mean-field treatment of strong-coupling Bose polaron in the mean-field limit). There is a well-known variational principle for the strong-coupling regime in which one starts with a variational ansatz for the impurity wavefunction [40, 41]. The impurity operators in the total Hamiltonian are then substituted by their expectation value over the variational state, leading to an effective Hamiltonian for the phonons. The ground state of the effective phonon Hamiltonian is then obtained assuming a coherent state for phonons. The so obtained ground state energy is then minimized with respect to the parameters of the impurity wavefunction.

In order to address the problem of topological polarons variationally, we pursue a slightly different path. More specifically, since we do not deal with a single impurity but rather a coherent state of impurities, we choose a coherent state variational ansatz for both boson and impurity fields. Taking the expectation value of the Hamiltonian over the impurity coherent state and minimizing for the effective bosons energy leads to Eq. (S23). The variational principle outlined for the strong-coupling Bose polaron suggests that, by solving for the bosons coherent state from Eq. (S23), we insert back the fields in the Hamiltonian, and minimize the energy functional with respect to the impurity variational parameters. However, this procedure has to be modified for our case since we are dealing with an interacting impurity field, not a single impurity (for which interaction terms in the Hamiltonian does not have any effects). In other words, our variational principle has to account for Eq. (S24) as well. We instead solve the set of simplified Eqs. (S25) and (S26) variationally. We follow the same procedure as the variational principle for solving the strong-coupling Bose polaron, with the extra modification that we now also have to account for Eq. (S26). In order to self-consistently account for this equation, first, we choose the two fields σ^0 and ϕ^0 to be proportional, $\sigma^0 \propto \phi^0$, and second, insert Eq. (S26) in Eq. (S25), which leads to minimizing the following energy functional for the field ϕ^0 only

$$H[\bar{\phi}^0, \phi^0] = \sum_{\mathbf{i}, \mathbf{j}} \bar{\phi}_{\mathbf{i}}^0 H_{\mathbf{i}\mathbf{j}}^{(\phi)} \phi_{\mathbf{j}}^0 - \frac{g}{2} \sum_{\mathbf{i}} (\bar{\phi}_{\mathbf{i}}^0 \phi_{\mathbf{i}}^0)^2 - \mu_{\phi} \left(\sum_{\mathbf{i}} \bar{\phi}_{\mathbf{i}}^0 \phi_{\mathbf{i}}^0 - N_{\phi} \right). \quad (\text{S27})$$

The energy functional in Eq. (S27) is just the original DNLS functional. In the next step, by the knowledge obtained from the soliton solutions of the DNLS in the main text, we assume that $\phi_{\mathbf{i}}^0$ belongs to a single band and expand it in terms of the Wannier functions of the corresponding band, $\phi_{\mathbf{i}}^0 = \sum_l a_l^{(n)} w^{(n)}(l)$. We then use a sech variational ansatz for the coefficient amplitudes, $a_l^{(n)} = \eta / \text{sech}(\xi(l - l_0))$. The variational energy functional takes the following form

$$H/\eta^2 = \omega_0 N_{\phi}/\eta^2 + \sum_{n=1}^{\infty} \frac{4n}{\sinh(\xi n)} \omega_n - \frac{2g}{3} \eta^2 \left[\frac{1}{\xi} + \sum_{m=1}^{\infty} \frac{2\pi^2}{\xi^2} \left(1 + \frac{\pi^2 m^2}{\xi^2} \right) \frac{m \cos(2\pi m l_0)}{\sinh(\frac{\pi^2 m}{\xi})} \right], \quad (\text{S28})$$

subject to the constraint $N_{\phi} = \text{const.}$, where

$$N_{\phi}/\eta^2 = \frac{2}{\xi} + \sum_{m=1}^{\infty} \frac{4\pi^2}{\xi^2} \frac{m \cos(2\pi m l_0)}{\sinh(\frac{\pi^2 m}{\xi})}. \quad (\text{S29})$$

For the simulations of the main text, we assume that $N_{\phi} = 1$. For more details on variational ansätze for DNLS consult [36, 54]. From the solution of Eqs. (S28) and (S29) we then obtain the boson field, $\phi_{\mathbf{i}}^0$, which is then used to obtain the impurity density $u_{\mathbf{i}}^0 = g \bar{\phi}_{\mathbf{i}}^0 \phi_{\mathbf{i}}^0$. The impurity density then acts as an effective attractive potential for bosons by virtue of Eq. (S25). By solving the associated eigenvalue problem, we obtain the Bose polaron as the bound state of the impurity potential, as depicted in Fig. (4) of the main text.

DERIVATION OF THE SOLITON CENTER-OF-MASS DISPLACEMENT

In this section we prove the quantized pumping of the soliton center-of-mass by the Chern number of the soliton band. For later convenience, we derive the following identity for matrix elements of position operator over the Wannier functions,

$$\begin{aligned} \langle w^{(n)}(l'), X w^{(n)}(l) \rangle &= \langle w^{(n)}(l' - l), (T_l^{\dagger} X T_l) w^{(n)}(0) \rangle \\ &= \langle w^{(n)}(l' - l), X w^{(n)}(0) \rangle + l \langle w^{(n)}(l' - l), w^{(n)}(0) \rangle \\ &= \langle w^{(n)}(l' - l), X w^{(n)}(0) \rangle + l \delta_{ll'} \end{aligned} \quad (\text{S30})$$

where T_l is the translation operator by l unit cells. In deriving Eq. (S30) we used the relation $T_l^\dagger X T_l = X + l$ together with the orthogonality of Wannier functions. The soliton center-of-mass then reads

$$\begin{aligned}
\langle \varphi^{(n)}, X \varphi^{(n)} \rangle_s &= \sum_{l, l'} a_{l'}^{(n)*} a_l^{(n)} \langle w^{(n)}(l'), X w^{(n)}(l) \rangle_s \\
&= \sum_l |a_l^{(n)}|^2 \langle w^{(n)}(l), X w^{(n)}(l) \rangle_s + \sum_{l \neq l'} a_{l'}^{(n)*} a_l^{(n)} \langle w^{(n)}(l'), X w^{(n)}(l) \rangle_s \\
&= \left(\sum_l |a_l^{(n)}|^2 \right) \langle w^{(n)}(0), X w^{(n)}(0) \rangle_s + \left(\sum_l |a_l^{(n)}|^2 l \right) \langle w^{(n)}(0), w^{(n)}(0) \rangle_s \\
&\quad + \sum_{\delta l \neq 0} \left(\sum_l a_{l+\delta l}^{(n)*} a_l^{(n)} \right) \langle w^{(n)}(\delta l), X w^{(n)}(0) \rangle_s,
\end{aligned} \tag{S31}$$

where we used Eq. (S30) in the last equality. The first term in the last equality in Eq. (S31) reduces to $\langle w^{(n)}(0), X w^{(n)}(0) \rangle_s$ since we normalized the soliton intensity to unity, $N_\phi = \sum_l |a_l^{(n)}|^2 = 1$. The second term in the last expression is the mean value of the position of the Wannier indices which is constant since the on-site solution is always peaked around a Wannier label and remains symmetric around it. Its contribution to the displacement over a pump cycle thus vanishes. The third term contains products of the form $(\sum_l a_{l+\delta l}^{(n)*} a_l^{(n)}) \times \langle w^{(n)}(\delta l), X w^{(n)}(0) \rangle_s$ and its treatment requires more care. The coefficient $(\sum_l a_{l+\delta l}^{(n)*} a_l^{(n)})$ is time-periodic, since $a_l^{(n)}$ by assumption is the solution of the scalar DNLS Eq. (6) in the main text. To investigate the behavior of $\langle w^{(n)}(\delta l), X w^{(n)}(0) \rangle_s$, we note that after a pump cycle, the Wannier functions are displaced by the Chern number, $w^{(n)}(l)|_{s=1} = w^{(n)}(l + \mathcal{C}_n)|_{s=0}$, with \mathcal{C}_n the Chern number of band n . Thus, after a pump cycle, we have

$$\langle w^{(n)}(\delta l), X w^{(n)}(0) \rangle_{s=1} = \langle w^{(n)}(\delta l + \mathcal{C}_n), X w^{(n)}(\mathcal{C}_n) \rangle_{s=0} = \langle w^{(n)}(\delta l), X w^{(n)}(0) \rangle_{s=0}. \tag{S32}$$

In the last equality, we used Eq. (S30). This means that $\langle w^{(n)}(\delta l), X w^{(n)}(0) \rangle_s$ is a periodic quantity. Thus, the third term in Eq. (S31) is also periodic, and the soliton center-of-mass displacement over a pump cycle is

$$\Delta \langle \varphi^{(n)}, X \varphi^{(n)} \rangle = \Delta \langle w^{(n)}(0), X w^{(n)}(0) \rangle, \tag{S33}$$

This proves the pumping of the soliton by the Chern number [38].